ELSEVIER

Journal of Chromatography A, 791 (1997) 85–98

JOURNAL OF CHROMATOGRAPHY A

Effect of mobile phase on the oligomerization state of α-helical coiled-coil peptides during high-performance size-exclusion chromatography

C.T. Mant[a], H. Chao[b], R.S. Hodges[a,b,*]

[a]*Department of Biochemistry and the Medical Research Council of Canada Group in Protein Structure and Function, University of Alberta, Edmonton, Alberta T6G 2H7, Canada*

[b]*Protein Engineering Network of Centres of Excellence, University of Alberta, Edmonton, Alberta T6G 2S2, Canada*

Received 7 April 1997; received in revised form 1 July 1997; accepted 4 July 1997

Abstract

Important structural motifs involving amphipathic helices include two-stranded and multiple-stranded coiled-coils. High-performance size-exclusion chromatography (HPSEC) is a useful tool to examine both the oligomerization state of coiled-coils as well as the stability of such motifs, due to the facile manipulation of the mobile phase and the lack of interaction of the peptide solutes with the stationary phase. In the present study, HPSEC was applied to two series of de novo designed model amphipathic α-helical peptides with the sequences (1) Ac–(E–A–L–K–A–E–I)$_n$–E–A–C–K–A–amide, where n=1 or 3, Ac–E–I–(E–A–L–K–A–E–I)$_4$–E–A–C–K–A–amide and (2) Ac–(K–L–E–A–L–E–A)$_n$–amide, where n=1, 2 or 4. Observation of the retention behaviour of Series 1 under both denaturing and non-denaturing conditions at pH 7.0 offered insights into the effect of polypeptide chain length and disulphide bridge formation on the stability of α-helical coiled-coils. In contrast, the Series 2 peptides showed promise as peptide standards to monitor the effect of environment on the multi-strandedness of coiled-coils, since the 28-residue peptide of this series was eluted as a monomer, dimer or trimer depending on mobile phase conditions.

Keywords: Mobile phase composition; Oligmerization state; Peptides; α-Helical coiled-coil peptides

1. Introduction

Inter-chain interactions are the main features responsible for the folding and stabilization of the three-dimensional structure of proteins, with amphipathic α-helices playing a vital role in hydrophobic interactions [1]. Indeed, about 50% of all α-helices in globular proteins are amphipathic [2] and such structures are also found in many fibrous proteins [1,3–6]. Important structural motifs involving such amphipathic α-helices include two-stranded and multiple-stranded (or multiple helix) coiled-coils [1].

While the study of single-stranded amphipathic α-helices reveals the effects of amino acid side-chains on intra-chain interactions, determining the effect on inter-chain interactions requires the pres-

*Corresponding author. Address for correspondence: Department of Biochemistry and the Medical Research Council of Canada Group in Protein Structure and Function, University of Alberta, Edmonton, Alberta T6G 2H7, Canada.

0021-9673/97/$17.00
PII S0021-9673(97)00767-X

ence of at least two interacting helices. The simplest model for such studies is well represented by the two-stranded α-helical coiled-coil motif [4,7]; in fact, the de novo design and synthesis of α-helical coiled-coils provides an ideal model system to study the importance of amphipathic α-helices for protein stability. This laboratory designed and synthesized by solid-phase peptide chemistry the first model coiled-coil protein and demonstrated its utility for studying folding and stability of α-helical proteins [8]. This early model has since been subject to continuing development in this laboratory, leading to a considerable body of published work on the universal dimerization domain represented by the two-stranded α-helical coiled-coil [9–33]; such work has also been extended to the formation of model four-stranded α-helical coiled-coils [28,30].

During any investigation involving model proteins with the potential for significant inter-chain interactions, such as the de novo coiled-coil systems noted above, it is important to obtain knowledge about the oligomerization state of the protein brought about by (1) the environment surrounding the protein or (2) manipulation of the length and/or sequence of the model protein. To this end, high-performance size-exclusion chromatography (HPSEC) has proved a particularly rapid and facile approach to monitoring the oligomerization state of synthetic coiled-coil peptides. Thus, Lau et al. [9,10] utilized HPSEC to examine the monomeric-dimeric structure of model peptides in various denaturing and non-denaturing mobile phases. Monera et al. [16] followed the effect of mobile phase conditions on the monomeric, dimeric and trimeric conformers, as well as higher aggregation states, of coiled-coil peptides. Zhou et al. [18], Zhu et al. [19], Monera et al. [30] and Fairman et al. [34] all monitored the formation of two-stranded versus four-stranded α-helical coiled-coils by HPSEC. A study by Kohn et al. [25] included monitoring the effect of pH on monomer versus dimer formation of two-stranded α-helical coiled-coils. An interesting study by Houston, Jr. et al. [35] employed HPSEC to determine the conformational states of lactam-bridged stabilized amphipathic α-helices.

A common thread which ran through many of the above studies was the recognition of the value of internal peptide standards to reflect the various oligomeric states of the peptides of interest. This laboratory has had considerable experience in the design and synthesis of peptide standards for the major modes of high-performance liquid chromatography (HPLC) [36,37], including HPSEC [37–39]. The aforementioned size-exclusion standards were designed to exhibit negligible secondary structure under any mobile phase conditions employed [38,39]. In contrast, the present study demonstrates the value of two series of synthetic model amphipathic α-helical peptide standards acting either as monitors of the effects of mobile phase conditions on the oligomeric states of α-helical coiled-coil peptides or as peptide conformation calibration standards for size-exclusion chromatography (SEC).

2. Experimental

2.1. Materials

HPLC-grade water was obtained from BDH (Poole, UK). Potassium chloride (KCl), potassium dihydrogenphosphate (KH_2PO_4) and urea (all reagent grade) were also obtained from BDH. The KH_2PO_4 solution was treated with BioRad Chelex-100 (BioRad, Richmond, CA, USA) chelating resin and passed through a 0.22-μm filter before use; the urea solution was treated with Bio-Rad AG 501-X8 (20–50 mesh) mixed-bed resin and passed through a 0.22-μm filter before use [40]. Trifluoroethanol (TFE) was obtained from Sigma (St. Louis, MO, USA).

2.2. Instrumentation

Peptide synthesis was carried out on an Applied Biosystems peptide synthesizer Model 430A (Foster City, CA, USA). Crude peptides were purified by an Applied Biosystems 400 solvent-delivery system connected to a 783A programmable absorbance detector.

The analytical HPLC system consisted of a Varian Vista Series 5000 liquid chromatograph (Varian, Walnut Creek, CA, USA) coupled to a Hewlett-Packard (Avondale, PA, USA), HP1040A detection system, HP9000 Series 300 computer, HP9133 disc

drive, HP2225A Thinkjet printer and HP7460A plotter.

Amino acid analyses of purified peptides were carried out on a Beckman Model 6300 amino acid analyzer (Beckman Instruments, Fullerton, CA, USA).

The correct primary ion molecular masses of peptides were confirmed by electrospray mass spectrometry on a Fisons Quattro (Fisons, Pointe-Claire, Quebec, Canada).

Circular dichroism (CD) spectra were recorded with a Jasco J-500C spectropolarimeter (Jasco, Easton, MD, USA) equipped with a Jasco IF500 II interface linked to an IBM PS/2 computer running the Jasco DP-500/PS2 system software (Version 1.33a). The temperature of the cuvette holder was controlled by a Lauda Model RMS water bath (Brinkman Instruments, Rexdale, ON, Canada). The spectropolarimeter was calibrated with an aqueous solution of recrystallized $d_{10}(+)$-camphorsulphonic acid at 290.5 nm.

Sedimentation equilibrium experiments were performed on a Beckman Model E analytical ultracentrifuge equipped with electronic speed control and Rayleigh interference optics.

2.3. Peptide synthesis

Amphipathic α-helical peptides were synthesized by the solid-phase technique (SPPS) on co-poly-(styrene-1% divinylbenzene)benzhydrylamine-hydrochloride resin (0.92 mmol/g resin) as previously described [41]. The HF-cleaved peptide-resin mixtures were washed with diethyl ether (3×25 ml) and the peptides extracted with neat acetic acid (3×25 ml) [41]. The resulting peptide solutions were then lyophilized prior to purification.

2.4. Columns

Crude peptides were purified on a semi-preparative SynChropak RP-P C_{18} reversed-phase column (250×10 mm I.D., 6.5 μm particle size, 300 Å pore size) from SynChrom (Lafayette, IN, USA). The peptides were purified at pH 2 by linear AB gradient elution (0.5% B/min) at a flow-rate of 5 ml/min, where eluent A is 0.1% aqueous trifluoroacetic acid (TFA) and eluent B is 0.1% TFA in acetonitrile.

Two size-exclusion columns were used: (1) Superdex 75 HR 10/30 (separation range, 3000—70 000 for globular proteins); (2) Superdex Peptide HR 10/30 (separation range, 100–7000). Both columns were obtained from Pharmacia Biotech (Baie d'Urfé, Québec, Canada).

2.5. HPSEC conditions

Four sets of mobile phase conditions were employed: mobile phase 1, 50 m*M* aqueous KH_2PO_4, containing 100 m*M* KCl, pH 7.0; mobile phase 2 was mobile phase 1 containing 30% (v/v) TFE; mobile phase 3 was mobile phase 1 containing 50% TFE; mobile phase 4 was mobile phase 1 containing 8 *M* urea. Flow-rates of 0.2 ml/min or 0.5 ml/min were used.

2.6. S-Carboxamidomethylation (alkylation) of peptide SH groups

Individual peptides were dissolved (1 mg/ml) in a highly denaturing buffer consisting of 50 m*M* KH_2PO_4, pH 7.0, containing 8 *M* guanidine hydrochloride. Dithiothreitol (DTT) was now added to a final concentration of 2 m*M* to ensure that the Cys residues remained in their sulphydryl forms. A solution of freshly prepared iodoacetamide (50 m*M*) in the same buffer was added to the peptide solution to a final concentration of 8 m*M*. The reaction mixture was stirred slowly for 30 min, followed by the addition of solid DTT to a final concentration of 20 m*M* to quench the excess iodoacetamide. The alkylated peptides were desalted/purified by reversed-phase chromatography employing a linear AB gradient and 0.1% aq. TFA–acetonitrile mobile phase (1% acetonitrile/min, 1 ml/min). The expected masses of the alkylated peptides were subsequently confirmed by mass spectrometry (MS).

2.7. Circular dichroism spectroscopy

CD runs were carried out as described by Chao et al. [32]. Measurements were made under non-denaturing conditions (50 m*M* phosphate buffer, pH 7.0, containing 100 m*M* KCl) at a temperature of 20°C.

2.8. Sedimentation equilibrium ultracentrifugation

Sedimentation equilibrium experiments were run under the same buffer and temperature conditions as those used for the CD runs. A total of five runs (48 h per run) was made with samples (100-μl aliquot) loaded at initial protein concentrations of 0.79 mg/ml (28K rpm), 1.59 mg/ml (28K rpm), 1.96 mg/ml (24K rpm) and 5.10 mg/ml (18K rpm and 22K rpm). Data collection and evaluation were carried out as described by Chao et al. [32].

3. Results and discussion

Two series of model synthetic peptide standards were employed in the present study. Both series of model peptides were based on a repeating heptad sequence $(a–b–c–d–e–f–g)_n$, containing hydrophobic residues at positions a and d, characteristic of two-stranded α-helical coiled-coil proteins [5,6]. The resulting sequence, $(N–X–X–N–X–X–X)_n$, where N is a non-polar residue, is known as a 3–4 or 4–3 repeat and was first identified by Sodek et al. [5].

3.1. Monitoring the effect of peptide chain length and disulphide-bridge formation on coiled-coil stability

3.1.1. Synthetic model peptides: Series 1

The peptides shown in Fig. 1 (Series 1) have previously been employed to study the effects of peptide chain length on the formation and stability of synthetic α-helical coiled-coils [21]. In the design of these peptides, several features were incorporated that are known to stabilize α-helices and coiled-coils. These features are highlighted in the schematic representation of the two-stranded α-helical coiled-coil formed by the dimerization of the 35-residue peptide (Fig. 1). Thus, for particular positions (c and f), alanine was selected because of its high intrinsic helical propensity [42–45]. The five residues used in the sequence (Ala, Glu, Ile, Lys and Leu) are the amino acids most frequently found in the heptad repeat of native proteins [7]. Analysis of coiled-coil sequences have shown that β-branched amino acids are generally preferred at hydrophobic position a, while leucine residues are usually found at hydrophobic position d [7,19,46,47]; hence, the choice of isoleucine and leucine at positions a and d, respectively, of the heptad. Finally, the hydrophilic charged amino acids lysine and glutamic acid were chosen and placed at positions of the peptide so that intramolecular electrostatic attractions were incorporated. From the schematic representation shown in Fig. 1, glutamate–lysine ion pairs are located in the i and $i+3$ (b–e) or i and $i+4$ (e–b) positions along the sequence, providing additional stability to the α-helical structure by side-chain electrostatic interactions [48–50]. Although the bulk of the interaction at the interface of the coiled-coil is hydrophobic (d–d′ and a–a′, Leu–Leu and Ile–Ile interactions, respectively), inter-chain electrostatic interactions between Glu and Lys in the i to $i'+5$ (e–g′ and e′–g) positions [16,22,51,52] provide further stability to the coiled-coil.

The α-helical potential of these Series 1 peptides has previously been reported [21]. Thus, in the presence of 50% (v/v) TFE, a widely used inert α-helix-inducing cosolvent [53,54], the α-helical content of the monomeric forms of the peptides was calculated to be 68.1%, 87.9% and 91.2% for peptides 12M, 26M and 35M, respectively [21].

The peptides denoted 52D and 70D (Fig. 1) represented the coiled-coil dimers of peptide 26M and 35M, respectively. The Cys residues of these monomeric peptides (as well as peptide 12M) have been reduced and treated with iodoacetamide (see Section 2.6) to prevent Cys oxidation and undesired disulphide bridge formation. The lack of a dimeric form for the 12-residue peptide, 12M, reflects the findings of Su et al. [21] that a minimum of three heptads was required for a peptide to adopt the two-stranded α-helical coiled-coil conformation in aqueous medium.

Finally, the presence of the Cys residue towards the C-terminal end of these peptides allows the formation of inter-chain disulphide bridges, the 12-residue, 26-residue and 35-residue peptides forming, respectively, 24-residue (denoted 24_0), 52-residue (52_0) and 70-residue (70_0) two-stranded peptides. Such two-stranded peptides are useful for monitoring by HPSEC the contribution to coiled-coil stability (peptides 52_0 and 70_0) of a disulphide bridge.

Peptide Denotion	Peptide Sequence	Monomeric MW
12M / 24_o	*b c d e f g a* Ac-(E-A-L-K-A-E-I)$_1$-E-A-C(X)-K-A-amide	1317 (12 M)
26M / 52D / 52_o	Ac-(E-A-L-K-A-E-I)$_3$-E-A-C(X)-K-A-amide	2826 (26 M)
35M / 70D / 70_o	Ac-E-I-(E-A-L-K-A-E-I)$_4$-E-A-C(X)-K-A-amide	3822 (35 M)

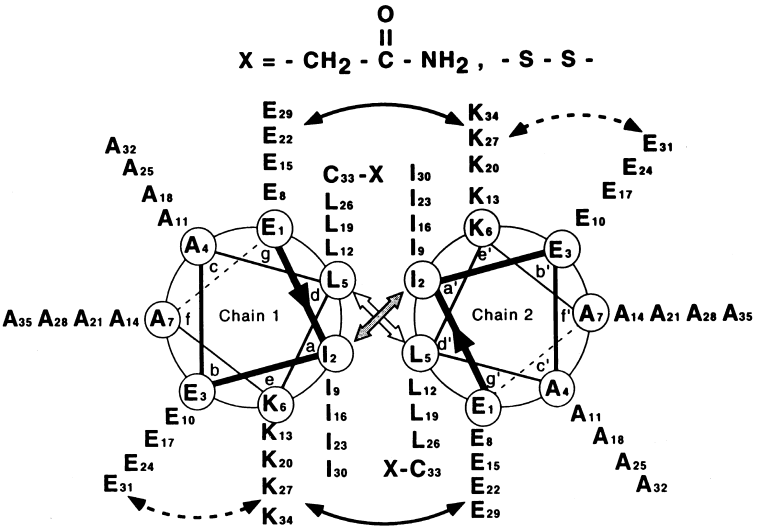

Fig. 1. Model peptide standards: Series 1. Top: sequences of model peptides (the single letter code for amino acids has been employed); Ac denotes N^{α}-acetyl and amide denotes C^{α}-amide. The X on the cysteine residue denotes that the sulphydryl side-chain has either been blocked (alkylated) with iodoacetamide (see Section 2.6) or has been oxidized to form a two-stranded disulphide-bridged species. The letters a–g denote positions in the repeating heptad (in parentheses) characteristic of coiled-coils. 12M, 26M and 35M denote the monomeric (alkylated) forms of the peptides; 52D and 70D denote the dimeric coiled-coils of 26M and 35M, respectively; 24_0, 52_0 and 70_0 denote the two-stranded, disulphide-bridged forms of the peptides. Bottom: schematic representation of two-stranded, α-helical coiled-coil formed by the dimerization of the 35-residue peptide. The chains are in register and parallel. The letters a to g and a′ to g′ designate the positions in the heptad repeat. The number following the capital letter indicates the position of that amino acid residue in the peptide sequence starting from the N-terminal end. The hydrophobic residues at a and a′ and d and d′ interact and are mainly responsible for the formation and stabilization of the coiled-coil. Electrostatic attractions could occur betwen b and e (b′ and e′), i.e., *i*, *i*+3 intra-chain interactions, or e and b (e′ and b′), i.e., i, *i*+4 intra-chain interactions (dashed arrows). Inter-chain interactions *i*, *i*′+5 (electrostatic attractions) (g–e′ or g′–e) are indicated by the solid arrows.

3.1.2. HPSEC elution behaviour of Series 1 peptides

Fig. 2 summarizes results obtained from HPSEC on the Superdex 75 column of mixtures of oxidized and reduced/alkylated peptides from Series 1 (Fig. 1) under non-denaturing conditions. The top panel shows the elution profile of the oxidized peptides (24_0, 52_0 and 70_0), demonstrating a satisfactory column performance. The bottom panel illustrates the relationship between $\log_{10} M_r$ and distribution coefficient (K_d) for both the oxidized and reduced/alkylated peptides shown in Fig. 1. The plot shows a good correlation for the three two-stranded disulphide-bridged peptides (24_0, 52_0 and 70_0) together with the alkylated 26- and 35-residue peptides (26M and 35M, respectively) when plotted as dimers (52D

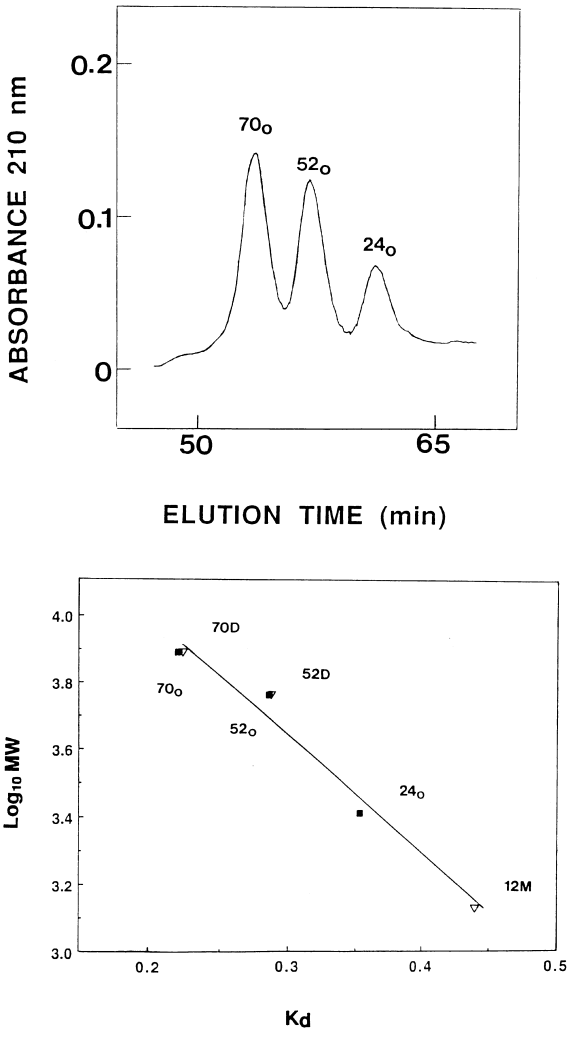

Fig. 2. Top: HPSEC elution profile of peptides 24_0, 52_0 and 70_0 (see Fig. 1) on Superdex 75 under non-denaturing conditions (mobile phase 1 in Section 2.5; flow-rate, 0.2 ml/min. Bottom: relationship between $\log_{10} M_r$ and distribution coefficient (K_d) for Series 1 peptide standards (see Fig. 1) eluted under non-denaturing conditions at a flow-rate of 0.2 ml/min. The K_d values were calculated from the expression $K_d = V_e - V_0 / V_t - V_0$, where V_e is the elution volume of the solute, V_0 is the void volume of the packing (obtained from the elution time of blue dextran) and V_t is the total accessible volume of the column (obtained from the elution time of β-mercaptoethanol).

and 70D, respectively). Thus, under these non-denaturing mobile phase conditions, both the 26M and 35M peptides are forming stable coiled-coil dimers (52D and 70D, respectively), supporting a previous report by Su et al. [21]. Only the alkylated 12-residue peptide was eluted as a monomer (12M) since, as noted previously, this peptide does not contain enough repeating heptads to form a stable coiled-coil, even under non-denaturing conditions.

It is interesting to note that the disulphide-bridged 24-mer (24_0), despite the unlikelihood of any significant coiled-coil character (notwithstanding the presence of the inter-chain disulphide bridge), still exhibited good correlation in its elution behaviour when compared to the dimeric (52D, 70D) and two-stranded (52_0, 70_0) coiled-coil peptides. These coiled-coil species would perhaps be expected to have a smaller molecular volume (rigid, rod-like molecules with high length/diameter ratio) than a less rigid, more unfolded molecule such as would be expected of peptide 24_0. However, it is possible that the presence of the disulphide bridge in peptide 24_0 put constraints enough on the two-stranded peptide (which also exhibited some α-helical potential [21]) to allow its retention behaviour to correlate well with the coiled-coil forms of the larger peptides.

Fig. 3 now shows the relationship between $\log_{10} M_r$ and K_d for the Series 1 peptides following

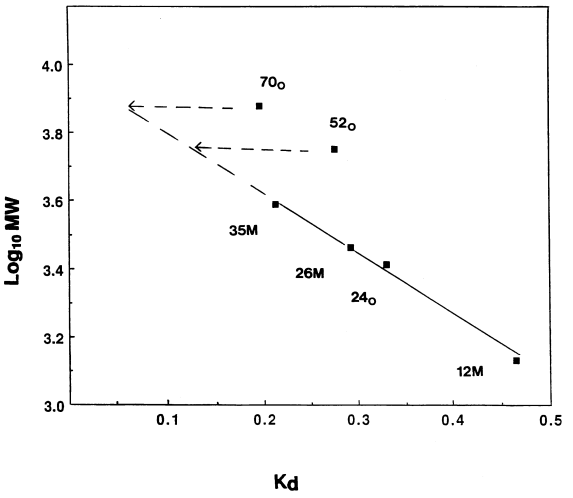

Fig. 3. Relationship between $\log_{10} M_r$ and K_d for Series 1 peptide standards (see Fig. 1) eluted from the Superdex 75 under highly denaturing conditions (8 *M* urea; mobile phase 4 in Section 2.5) at a flow-rate of 0.2 ml/min. K_d values were calculated as shown in Fig. 3. The arrows and dotted lines denote the expected elution positions of peptides 52_0 and 70_0 if they were in the same conformational state as the other peptides.

HPSEC on the Superdex 75 column in the presence of 8 *M* urea, i.e., under conditions highly denaturing to folded peptides/proteins. The reduced/alkylated peptides all now run as monomeric species (12M, 26M, 35M), since the highly denaturing conditions have disrupted the dimeric state of peptides 26M and 35M (denoted 52D and 70D, respectively, in Figs. 1 and 2) and they are almost certainly being eluted as random coils, i.e., all secondary and quaternary structure has been disrupted. In addition, the good correlation of oxidized, two-stranded peptide 24_0 with the three monomers suggests that all four of the peptides are behaving as random coils.

The elution behaviour of the other two-stranded peptides (peptides 52_0 and 70_0) is much different than that of the peptide 24_0 analogue. From Fig. 3, the arrows and dashed lines denote where it may have been expected to observe peptides 52_0 and 70_0 to be eluted if they were in the same conformational state (i.e., random coil) as the other peptides. These two peptides are being retained by the column longer than would have been expected, i.e., they are behaving as smaller molecules than expected, suggesting their conformation is still that of coiled-coil peptides rather than random coils. Thus, the disulphide bridge linking the two strands of these peptides is sufficient to stabilize the coiled-coil conformation of the peptides even under highly denaturing mobile phase conditions. Indeed, it is interesting to note how peptide 52_0 is being eluted later than a peptide (35M) with a lower-molecular-mass, due to the maintenance of peptide 52_0 as a small rod-like molecule in contrast to the now random coil peptide 35M. These results are in good agreement with previous studies concerning the contribution of disulphide bonds to de novo designed coiled-coil stability [18] and are a clear testament to the effectiveness of such bonds in maintaining such conformations even in highly denaturing environments.

3.2. Monitoring oligomerization state of model peptides by SEC

3.2.1. Model synthetic peptides: Series 2

The peptides shown in Fig. 4 were designed as standards to calibrate HPSEC columns for confirmation of monomeric versus multimeric peptide conformations for protein design studies. The general features concerning the sequences of the heptad repeats of these peptides are similar to those described for the Series 1 peptides (Fig. 1). Thus, both series of peptides contain Ala, Glu, Lys and Leu residues, with Ala again at positions c and f. However, only the peptide analogue with a total of four heptads (peptide 28M) is long enough to adopt a two-stranded α-helical coiled-coil (denoted peptide 56D) in aqueous medium, i.e., the 7-residue and 14-residue analogues (peptides 7M and 14M) are always in their monomeric forms. From the schematic representation of the dimeric coiled-coil form of peptide 28M, denoted 56D, in Fig. 4, it can be seen that the bulk of the interaction of the interface of the coiled-coil is again hydrophobic (d–d′ and a–a′, albeit now with two pairs of Leu–Leu interactions). In addition, inter-chain Glu–Lys electrostatic interactions (e–g′ and e′–g) are again possible, although it should be noted that the relative positions of these two residues has been reversed (Glu is now in position e and Lys in position g) compared to the Series 1 peptides (Fig. 1). Due to the positioning of Glu at position e in the sequence, as well as position b, there is now a possibility of intra-molecular repulsive forces (as opposed to the attractive forces seen in Fig. 1 for Series 1 peptides) between the i and $i+3$ (b–e) or i and $i+4$ (e–b) positions along the sequence. Unlike the Series 1 peptides, the Series 2 analogue capable of forming a two-stranded coiled-coil (28M→56D; Fig. 4) was not designed to maximize coiled-coil stability. With this approach, it was intended that the oligomerization state of the 28-residue analogue of the Series 2 model peptides would be more subtly influenced by its environment.

The α-helical potential of peptide analogues almost identical to the Series 2 peptides (save for an Ala→Gly substitution at position f of the heptad) has been previously documented [9,10]. In addition, the coiled-coil potential of the present 28-residue standard has been confirmed in the present study by CD and sedimentation equilibrium studies and will be discussed later.

3.2.2. HPSEC elution behaviour of Series 2 peptides

Fig. 5 shows the relationship between $\log_{10} M_r$

Peptide Denotion	Peptide Sequence	Monomeric MW
	g a b c d e f	
7M	Ac-(K-L-E-A-L-E-A)$_1$-amide	814
14M	Ac-(K-L-E-A-L-E-A)$_2$-amide	1569
28M / 56D / 84T	Ac-(K-L-E-A-L-E-A)$_4$-amide	3078

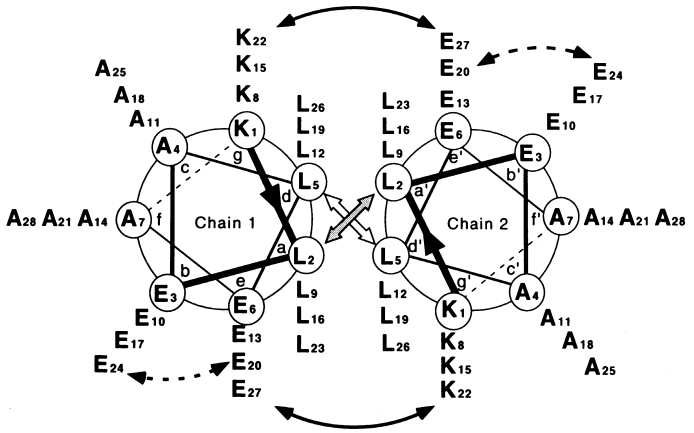

Fig. 4. Model peptide standards: Series 2. Top: sequences of model peptides (the single letter code for amino acids has been employed); Ac denotes N^{α}-acetyl and amide denotes C^{α}-amide. The letters a–g denote positions in the repeating heptad (in parentheses) characteristic of coiled-coils. 7M, 14M and 28M denote the monomeric forms of the peptides; 56D and 84T denote, respectively, the dimeric and trimeric coiled-coil forms of 28M. Bottom: schematic representation of two-stranded, α-helical coiled-coil formed by the dimerization of the 28-residue peptide. The chains are in register and parallel. The letters a to g and a′ to g′ designate the positions in the heptad repeat. The number following the capital letter indicates the position of that amino acid residue in the peptide sequence starting from the N-terminal end. The hydrophobic residues at a and a′ and d and d′ interact and are mainly responsible for the formation and stabilization of the coiled-coil. Electrostatic repulsion could occur betwen b and e (b′ and e′), i.e., *i*, *i*+3 intra-chain interactions, or e and b (e′ and b′), i.e., *i*, *i*+4 intra-chain interactions (dashed arrows). Inter-chain interactions *i*, *i*′+5 (electrostatic attractions) (g–e′ or g′–e) are indicated by the solid arrows.

and K_d for the Series 2 peptides following HPSEC on the Superdex 75 column in the presence of 8 *M* urea (Fig. 5, top), 50% TFE (Fig. 5, middle) and 30% TFE (Fig. 5, bottom) (mobile phases 4, 3 and 2, respectively; see Section 2.5).

Under the highly denaturing conditions characteristic of the presence of 8 *M* urea (Fig. 5, top), the three peptides, as expected, are all eluted as single-stranded (and random-coil) species.

The effect of 50% TFE on the elution behaviour of the peptide standards (Fig. 5, middle) shows some similarities to those observed for the mobile phase containing 8 *M* urea (Fig. 5, top), but there are also important differences due to the α-helical promoting properties of TFE, albeit these differences are not immediately obvious from the $\log_{10} M_r$ versus K_d relationship shown in Fig. 5 (middle). Thus, TFE is a denaturant of quaternary structure but promotes α-helical structure in potentially helical molecules [9,55,56]. From Fig. 5 (middle), all three peptides are

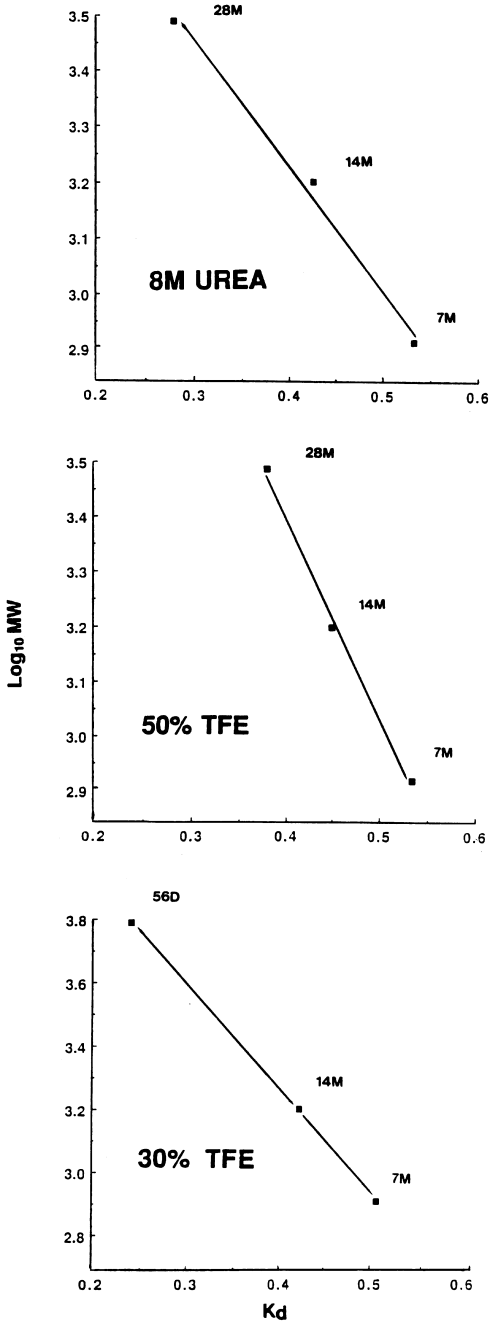

Fig. 5. Relationship between $\log_{10} M_r$ and K_d for Series 2 peptide standards (see Fig. 2) eluted from the Superdex 75 under various denaturing conditions at a flow-rate of 0.2 ml/min. The top, middle and bottom profiles show the results obtained using mobile phase 4 (8 *M* urea), mobile phase 3 (50% TFE) and mobile phase 2 (30% TFE), respectively. The compositions of the mobile phases are shown in Section 2.5. K_d values were calculated as shown in Fig. 3.

being eluted as monomeric peptides, since the presence of 50% TFE in the mobile phase overcomes even the strong coiled-coil potential of the 28-residue standard. However, unlike the highly denaturing conditions of 8 *M* urea (Fig. 5, top), the presence of 50% TFE in the mobile phase ensures the peptides are being eluted in their monomeric helical forms as opposed to random coils.

Lowering the TFE concentration in the mobile phase to 30% (Fig. 5, bottom) now changes the elution behaviour of the 28-residue peptide, suggesting elution as a dimeric coiled-coil, denoted 56D, while the 7-residue and 14-residue peptides remain monomeric. This observation highlights the relative stability of the dimer produced by the four heptads of the 28-residue standard, since the coiled-coil is maintained even in the presence of a significant concentration of denaturant (30% TFE) of protein quaternary structure.

Fig. 6 (top) now shows the elution profile of the oxidized Series 1 peptides (24_0, 52_0, 70_0; Fig. 1) and the three Series 2 peptide standards (Fig. 4) under non-denaturing conditions, i.e., in the absence of TFE or urea; the $\log_{10} M_r$ versus K_d plot for the peptides shown in Fig. 6 (top) plus the non-oxidized (i.e., no inter-chain disulphide bridge) monomeric (12M) and dimeric (52D, 70D) Series 1 peptides is shown in Fig. 6 (bottom). Various mixtures of the peptides from both peptide series were run on the Superdex 75 column under these non-denaturing conditions and the plot shown in Fig. 6 (bottom) represents a summary of these runs. This was carried out in order to maximize the number of data points on the plot, and, hence, confirm the very interesting observation that the 28-residue peptide standard from the Series 2 peptides (Fig. 4) now appeared to exhibit a trimeric conformation, denoted 84T. The expected elution positions for the 28-residue peptide if eluted as a dimer (56D) or as a monomer (28M) are also indicated on the plot shown in Fig. 6 (bottom); the very poor correlation of these positions supported the assumption that the 28-mer standard was behaving as a trimer (denoted 84T). If this was indeed the case, then a new dimension has been added to the value of these calibration standards in that the oligomerization state of the largest peptide is particularly sensitive to mobile phase conditions. Thus, under highly denaturing conditions (Fig. 5, top

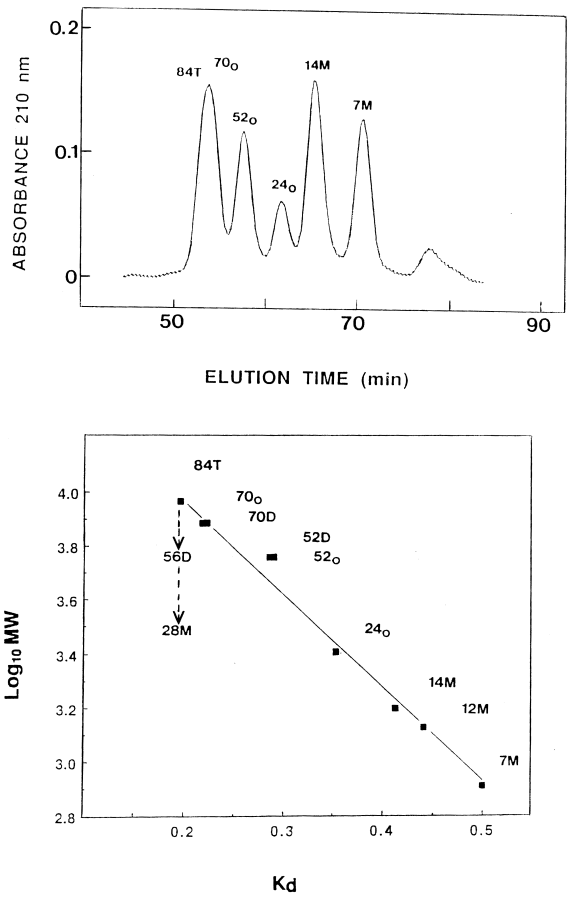

Fig. 6. Top: HPSEC elution profile of peptides 24_0, 52_0, 70_0 (see Fig. 1) and 7M, 14M, 84T (see Fig. 2) on Superdex 75 column under non-denaturing conditions (mobile phase 1 in Section 2.5) at a flow-rate of 0.2 ml/min. Bottom: relationship between $\log_{10} M_r$ and K_d for Series 1 (see Fig. 1) and Series 2 (see Fig. 2) peptide standards eluted under non-denaturing conditions at a flow-rate of 0.2 ml/min. Sample volume: 40 μl, containing the 28-residue peptide at a concentration of 1 mg/ml. The volume of the peak when eluted was 600 μl, i.e., an elution concentration for this peptide of 0.067 mg/ml. K_d values were calculated as shown in Fig. 3. The arrows and dotted lines denote the expected elution positions of the 28-residue peptide from Series 2 if it had been eluted as a monomer (28M) or dimer (56D).

and middle), the 28-mer was eluted in a monomeric form; under mildly denaturing conditions (Fig. 5, bottom), it was eluted as a dimer; and, finally, under non-denaturing conditions (Fig. 6), it appeared to be eluted as a trimer.

Due to the importance of this observation, it was necessary to obtain strong supportive evidence that the 28-residue could indeed form multi-stranded forms other than the dimeric coiled-coil form for which it was originally designed. Fortunately, such evidence could be readily located in the literature, since interest in de novo designed trimeric [57–67] and also tetrameric [28,30,59,68] model coiled-coil motifs has been steadily growing in recent years. Thus, the general principles of structural characteristics and interactions which stabilize dimeric coiled-coils (e.g., hydrophobic interactions at the interface of the individual peptide chains and potential intra-chain and inter-chain electrostatic interactions) may also be applied to more complex coiled-coil motifs. Indeed, efforts to predict different oligomerization states of coiled-coils [69,70] have centered around the heptad repeat first identified by Sodek et al. [5] as being responsible for dimeric coiled-coil structures. Significantly, it was noted by Lombardi et al. [64] that de novo designed peptides patterned after Hodges et al.'s original design of two-stranded coiled-coils [8] actually formed trimers in solution and in the solid state, this original design being almost identical to the heptad repeat of the peptide standards currently under discussion.

The oligomeric structure of the 28-residue peptide was now examined by sedimentation equilibrium ultracentrifugation experiments under non-denaturing conditions (see Section 2.8). Since it is difficult to analyze multimer-equilibrium from ultracentrifugation data, a total of five runs differing in loading concentrations and speeds (see Section 2.8) was performed, with the observed peptide distribution profile ranging from 0.34 mg/ml to 8.79 mg/ml. Although several good models were used to analyze the data globally, the only reasonable fit was obtained by the program NONLIN [71], which suggested that a trimer–tetramer model best described the data set. The monomeric or dimeric forms were not significantly observed and the data obtained could essentially be described in the absence of these species. These data suggested that the trimeric form did indeed predominate at concentrations below 1 mg/ml, such results being entirely consistent with the sample concentrations at the start of the HPSEC run as well as following dilution during elution from the column (see legend to Fig. 6 for details). Interestingly, the sedimentation equilibrium data indicated that the tetrameric oligomerization state of the

peptide became the dominant species at concentrations above 2 mg/ml. Higher order aggregates were not observed.

CD analysis of the 28-mer standard trimer (denoted 84T), indicated considerable helical structure. Thus, at 0.48 mg/ml, where the trimeric coiled-coil predominated in solution, the CD profile was consistent of a structure close to 100% helicity. This full helical structure was further corroborated by TFE titration experiments, where the presence of TFE at concentrations of 30% or 50% (v/v) did not increase or decrease helix content as indicated by the lack of CD signal intensity changes. These data supported the notion that the 28-residue standard could associate to form a stable coiled-coil under non-denaturing conditions and the monomeric species does not populate significantly even at low concentrations in agreement with the sedimentation equilibrium data.

3.3. Evaluation of size-exclusion columns by synthetic peptide standards

3.3.1. HPSEC of peptides on Superdex Peptide and Superdex 75 columns

Table 1 shows the sequences of synthetic peptides, ranging in length from 4 to 20 residues (~500–2200), used to evaluate the potential of the recently introduced Superdex Peptide size-exclusion column. The capabilities of the Superdex Peptide and Superdex 75 columns to resolve a mixture of these peptides under non-denaturing conditions (mobile phase 1; see Section 2.5) are compared in Fig. 7. The inability of the Superdex 75 column (top profile) to resolve these peptides is unsurprising, considering that the optimum fractionation range for the column is 3000–70 000 for globular proteins and, thus, these peptides represent a narrow-molecular-mass variation at the extreme low end of the resolving capability of the column. Indeed, these results are entirely consistent with previous observations by our laboratory when comparing the separations of synthetic peptide SEC standards (10–50 residues; 800–4000) on various columns designed for protein separations [38,39].

The excellent resolution of the six peptides shown in Table 1 achieved on the Superdex Peptide column (Fig. 7, middle profile) is a clear illustration of the potential of this column for small peptide separations. In fact, the resolving capability of the column should be even more advantageous for purification of complex peptide mixtures by a multistep process [36,72,73]. Thus, an initial fractionation of such a mixture by the Superdex Peptide column should simplify considerably subsequent ion-exchange chromatography and/or reversed-phase chromatography steps.

It should be noted that plotting the logarithm of the number of residues versus K_d (Fig. 7, bottom panel) gave a noticeably higher correlation ($r=0.995$) compared to a more traditional $\log_{10} M_r$ versus K_d plot ($r=0.972$). The lesser correlation of the latter plot was mainly apparent for the smallest peptides of 4 and 6 residues (Table 1), probably due to the lack of any defined shape (spherical or otherwise) of such small peptides.

3.3.2. HPSEC of synthetic amphipathic α-helical peptide standards on Superdex Peptide and Superdex 75 columns

Fig. 8 compares the elution behaviour of the model peptides shown in Fig. 4 on the Superdex 75

Table 1
Synthetic model peptides

Peptide sequence[a]	Number of residues	Molecular mass
F–I–P–K	4	504
Ac–G–G–T–A–G–G–amide	6	459
P–Q–S–P–E–S–V–D–amide	8	857
L–K–A–E–I–E–A–L–K–A–amide	10	1085
Ac–T–D–D–P–A–S–P–Q–S–P–E–S–V–D–amide	14	1483
I–E–A–L–K–C–E–I–E–A–L–K–A–E–I–E–A–L–K–A–amide	20	2186

[a] Peptide sequences are shown using the one letter code for amino acid residues; Ac denotes N^{α}-acetyl; amide=C^{α}-amide.

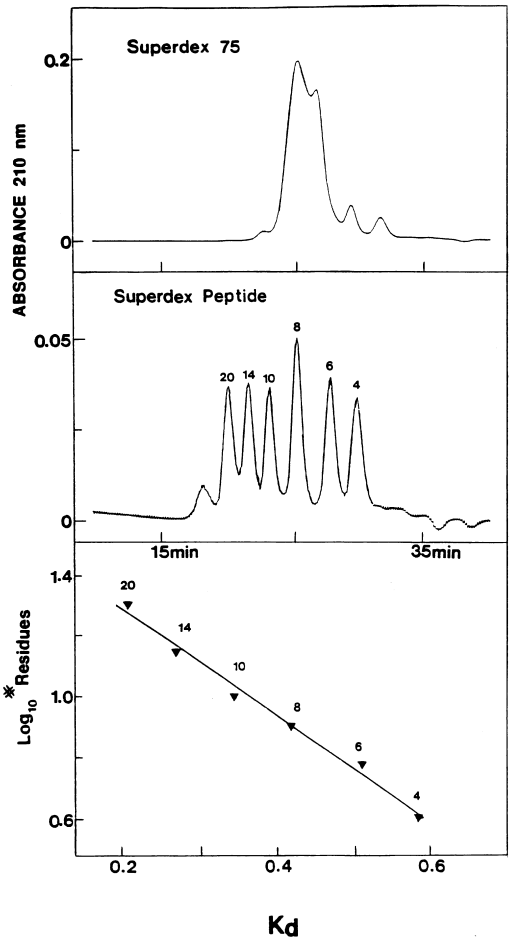

Fig. 7. HPSEC of small peptides on Superdex 75 (top) and Superdex Peptide (middle) columns under non-denaturing conditions (mobile phase 1 in Section 2.5) at a flow-rate of 0.5 ml/min. The bottom panel shows the resulting $\log_{10}$ Number of Residues versus K_d relationship. K_d values were calculated as shown in Fig. 3. The sequences of the peptides are shown in Table 1; the numbers above the peaks in the middle profile and on the bottom plot denote the number of residues in the peptides.

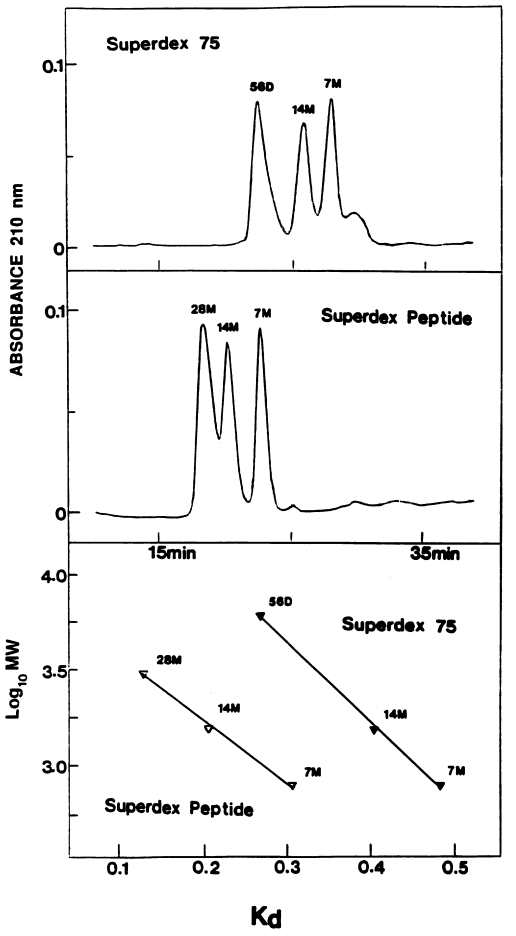

Fig. 8. Comparison of HPSEC of Series 2 peptide standards (see Fig. 2) on Superdex 75 (top profile) and Superdex Peptide (middle profile) columns in the presence of 30% TFE (mobile phase 2 in Section 2.5) at a flow-rate of 0.5 ml/min. The bottom panel compares the resulting $\log_{10} M_r$ versus K_d relationship on the two columns. K_d values were calculated as shown in Fig. 3.

(top profile) and Superdex Peptide (middle profile) columns in the presence of 30% TFE (mobile phase 2; see Section 2.5). The lower panel of Fig. 8 compares the $\log_{10} M_r$ versus K_d plots for the two columns. As was demonstrated earlier (Fig. 5, bottom), the 28-residue standard is eluted as a dimeric coiled-coil (denoted 56D in Fig. 4) on the Superdex 75 under these conditions. In contrast, this peptide is eluted in its monomeric form (denoted 28M in Fig. 4) on the Superdex Peptide column. Thus, the column matrix appears to be somehow influencing the oligomeric state of the 28-residue standard. This interesting observation further enhances the value of these calibration standards in that, in addition to being sensitive to mobile phase variations, the 28-residue peptide also appears to be sensitive to the particular SEC packing employed for its elution.

4. Conclusions

In this study, we have demonstrated that SEC is a

rapid and facile method for determining the oligomerization state of de novo designed amphipathic α-helical peptides. Thus, SEC under denaturing or non-denaturing conditions enabled a demonstration of the influence on coiled-coil stability of peptide chain length and intra-chain disulphide bridge formation. In addition, a series of model synthetic peptide size-exclusion standards designed to determine the influence of mobile phase on the oligomerization state of α-helical coiled-coils also demonstrated a useful monitoring function in their sensitivity to the characteristics of the particular size-exclusion column employed.

Acknowledgments

This work was supported by the Medical Research Council Group in Protein Structure and Function and by the Protein Engineering Network of Centres of Excellence. We thank Paul Semchuk for synthesizing the peptides used in this study.

References

[1] R.E. Epand (Editor), The Amphipathic Helix, CRC Press, Boca Raton, FL, 1991.
[2] J.L. Cornette, K.B. Cease, H. Margalit, J.L. Spouge, J.A. Berzofsky, C.D. DeLisi, J. Mol. Biol. 195 (1987) 659.
[3] F.H.C. Crick, Acta Crystallogr. 6 (1953) 689.
[4] C. Cohen, D.A.D. Parry, TIBS 11 (1986) 245.
[5] J. Sodek, R.S. Hodges, L.B. Smillie, L. Jurasek, Proc. Natl. Acad. Sci. USA 69 (1972) 3800.
[6] D. Stone, J. Sodek, P. Johnson, L.B. Smillie, Proc. 9th Fed. Eur. Biochem. Soc. Meet., Protein Contractile Syst. 31 (1975) 125.
[7] C. Cohen, D.A.D. Parry, Proteins: Struct. Function Gen. 7 (1990) 1.
[8] R.S. Hodges, A.K. Saund, P.C.S. Chong, S.A. St-Pierre, R.E. Reid, J. Biol. Chem. 256 (1981) 1214.
[9] S.Y.M. Lau, A.K. Taneja, R.S. Hodges, J. Biol. Chem. 259 (1984) 13253.
[10] S.Y.M. Lau, A.K. Taneja, R.S. Hodges, J. Chromatogr. 317 (1984) 129.
[11] R.S. Hodges, N.E. Zhou, C.M. Kay, P.D. Semchuk, Pept. Res. 3 (1990) 123.
[12] R.S. Hodges, Curr. Biol. 2 (1992) 122.
[13] N.E. Zhou, B.-Y. Zhu, C.M. Kay, R.S. Hodges, Biopolymers 32 (1992) 419.
[14] N.E. Zhou, C.M. Kay, R.S. Hodges, J. Biol. Chem. 267 (1992) 2664.
[15] N.E. Zhou, C.M. Kay, R.S. Hodges, Biochemistry 31 (1992) 5739.
[16] O.D. Monera, N.E. Zhou, C.M. Kay, R.S. Hodges, J. Biol. Chem. 268 (1993) 19218.
[17] J.G. Adamson, N.E. Zhou, R.S. Hodges, Curr. Opin. Biotechnol. 4 (1993) 428.
[18] N.E. Zhou, C.M. Kay, R.S. Hodges, Biochemistry 32 (1993) 3178.
[19] B.-Y. Zhu, N.E. Zhou, C.M. Kay, R.S. Hodges, Protein Sci. 2 (1993) 383.
[20] O.D. Monera, C.M. Kay, R.S. Hodges, Biochemistry 33 (1994) 3862.
[21] J.Y. Su, R.S. Hodges, C.M. Kay, Biochemistry 33 (1994) 15501.
[22] N.E. Zhou, C.M. Kay, R.S. Hodges, Protein Eng. 7 (1994) 1365.
[23] N.E. Zhou, C.M. Kay, R.S. Hodges, J. Mol. Biol. 237 (1994) 500.
[24] W.D. Kohn, C.M. Kay, R.S. Hodges, Protein Sci. 4 (1995) 237.
[25] W.D. Kohn, O.D. Monera, C.M. Kay, R.S. Hodges, J. Biol. Chem. 270 (1995) 25495.
[26] P. Lavigne, L.H. Kondejewski, M.E. Houston Jr., F.D. Sönnichsen, B. Lix, B.D. Sykes, R.S. Hodges, C.M. Kay, J. Mol. Biol. 254 (1995) 505.
[27] P. Lavigne, F.D. Sönnichsen, C.M. Kay, R.S. Hodges, J. Mol. Biol. 271 (1996) 1136.
[28] O.D. Monera, N.E. Zhou, P. Lavigne, C.M. Kay, R.S. Hodges, J. Biol. Chem. 271 (1996) 3995.
[29] R.S. Hodges, Biochem. Cell. Biol. 74 (1996) 133.
[30] O.D. Monera, F.D. Söonnichsen, L. Hicks, C.M. Kay, R.S. Hodges, Protein Eng. 9 (1996) 353.
[31] B.D. Tripet, L. Yu, D.L. Bautista, W.Y. Wong, R.T. Irvin, R.S. Hodges, Protein Eng. 9 (1996) 1029.
[32] H. Chao, M.E. Houston Jr., S. Grothe, C.M. Kay, M. O'Connor-McCourt, R.T. Irvin, R.S. Hodges, Biochemistry 35 (1996) 12175.
[33] M.E. Houston Jr., A. Wallace, E. Bianchi, A. Pessi, R.S. Hodges, J. Mol. Biol. 262 (1996) 270.
[34] R. Fairman, H.-G. Chao, L. Mueller, T.B. Lavoie, L. Shen, J. Novotny, G.R. Matsueda, Protein Sci. 4 (1995) 1457.
[35] M.E. Houston Jr., A.P. Campbell, B. Lix, C.M. Kay, B.D. Sykes, R.S. Hodges, Biochemistry 35 (1996) 10041.
[36] C.T. Mant and R.S. Hodges (Editors), High-Performance Liquid Chromatography of Peptides and Proteins: Separation, Analysis and Conformation, CRC Press, Boca Raton, FL, 1991.
[37] C.T. Mant, R.S. Hodges, Methods Enzymol. 271 (1996) 3.
[38] C.T. Mant, J.M.R. Parker, R.S. Hodges, J. Chromatogr. 397 (1987) 99.
[39] C.T. Mant and R.S. Hodges, in C.T. Mant and R.S. Hodges (Editors), High-Performance Liquid Chromatography of Peptides and Proteins: Separation, Analysis and Conformation, CRC Press, Boca Raton, FL, 1991, p. 225.
[40] C.T. Mant and R.S. Hodges, in C.T. Mant and R.S. Hodges (Editors), High-Performance Liquid Chromatography of Peptides and Proteins: Separation, Analysis and Conformation, CRC Press, Boca Raton, FL, 1991, p. 37.

[41] T.J. Sereda, C.T. Mant, A.M. Quinn, R.S. Hodges, J. Chromatogr. 646 (1993) 17.
[42] K.T. O'Neil, W.F. DeGrado, Science 250 (1990) 646.
[43] N.E. Zhou, O.D. Monera, C.M. Kay, R.S. Hodges, Protein Pep. Lett. 1 (1994) 114.
[44] A. Chakrabartty, T. Kortemme, R.L. Baldwin, Protein Sci. 3 (1994) 843.
[45] O.D. Monera, T.J. Sereda, N.E. Zhou, C.M. Kay, R.S. Hodges, J. Pep. Sci. 1 (1995) 319.
[46] S.L. McKnight, Sci. Am. 264 (1991) 54.
[47] J.C. Hu, R.T. Sauer, Nucleic Acids Mol. Biol. 6 (1992) 82.
[48] S. Marqusee, R.L. Baldwin, Proc. Natl. Acad. Sci. USA 84 (1987) 8898.
[49] G. Merutka, E. Stellwagen, Biochemistry 30 (1991) 1591.
[50] J.M. Scholtz, R.L. Baldwin, Annu. Rev. Biophys. Biomol. Struct. 21 (1992) 95.
[51] R.S. Hodges, P.D. Semchuk, A.K. Taneja, C.M. Kay, J.M.R. Parker, C.T. Mant, Pept. Res. 1 (1988) 19.
[52] K.S. Thompson, C.R. Vinson, E. Freire, Biochemistry 32 (1993) 5491.
[53] N. Lotan, A. Berger, E. Katchalski, Annu. Rev. Biochem. 41 (1972) 869.
[54] J.W. Nelson, N.R. Kallenbach, Biochemistry 28 (1989) 5256.
[55] T.M. Cooper, R.W. Woody, Biopolymers 30 (1990) 657.
[56] F.D. Sönnichsen, J.E. Van Eyk, R.S. Hodges, B.D. Sykes, Biochemistry 31 (1992) 8790.
[57] K. O'Neil, W.F. DeGrado, Science 250 (1990) 646.
[58] B. Lovejoy, S. Choe, D. Cascio, D.K. McRorie, W.F. DeGrado, D. Eisenberg, Science 259 (1993) 1288.
[59] P.B. Harbury, T. Zhang, P. Kim, T. Alber, Science 262 (1993) 1401.
[60] P.B. Harbury, P. Kim, T. Alber, Nature 371 (1994) 80.
[61] H. Wendt, C. Berger, A. Baici, R.M. Thomas, H.R. Bosshard, Biochemistry 34 (1995) 4097.
[62] S. Nautiyal, D.N. Woolfson, D.S. King, T. Alber, Biochemistry 34 (1995) 11645.
[63] S. Betz, R. Fairman, K. O'Neil, J. Lear, W.F. DeGrado, Phil. Trans. R. Soc. Lond. B 348 (1995) 81.
[64] A. Lombardi, J.W. Bryson, W.F. DeGrado, Peptide Sci. 40 (1996) 495.
[65] L. Gonzalez Jr., R.A. Brown, D. Richardson, T. Alber, Nature Struc. Biol. 3 (1996) 1002.
[66] J. Boice, G.R. Dieckmann, W.F. DeGrado, R. Fairman, Biochemistry 35 (1996) 14480.
[67] N.L. Ogihara, M.S. Weiss, W.F. DeGrado, D. Eisenberg, Protein Sci. 6 (1997) 80.
[68] R. Fairman, H.-G. Chao, L. Mueller, T.B. Lavoie, L. Shen, J. Novotny, G.R. Matsueda, Protein Sci. 4 (1995) 1457.
[69] W.L. DeLano, A.T. Brünger, Proteins: Struc. Func. Gen. 20 (1994) 105.
[70] D.N. Woolfson, T. Alber, Protein Sci. 4 (1995) 1596.
[71] M.L. Johnson, J.J. Correia, D.A. Yphantis, H.R. Halvorson, Biophys. J. 36 (1981) 575.
[72] C.T. Mant, R.S. Hodges, J. Chromatogr. 326 (1985) 349.
[73] C.T. Mant, R.S. Hodges, J. Liq. Chromatogr. 12 (1989) 139.